



TITLE:

Energy transfer in mixed CdSe and Au nanoparticle monolayers studied by simultaneous photoluminescence and Raman spectral measurements

AUTHOR(S):

Kawai, Masaki; Yamamoto, Aishi; Matsuura, Norihiro; Kanemitsu, Yoshihiko

CITATION:

Kawai, Masaki ...[et al]. Energy transfer in mixed CdSe and Au nanoparticle monolayers studied by simultaneous photoluminescence and Raman spectral measurements. Physical Review B 2008, 78(15): 153308.

ISSUE DATE:

2008-10

URL:

<http://hdl.handle.net/2433/87348>

RIGHT:

c 2008 The American Physical Society

Energy transfer in mixed CdSe and Au nanoparticle monolayers studied by simultaneous photoluminescence and Raman spectral measurements

Masaki Kawai,¹ Aishi Yamamoto,^{1,*} Norihiro Matsuura,¹ and Yoshihiko Kanemitsu^{2,3,†}

¹*Graduate School of Materials Science, Nara Institute of Science and Technology, Ikoma, Nara 630-0192, Japan*

²*Institute for Chemical Research, Kyoto University, Uji, Kyoto 611-0011, Japan*

³*Photonics and Electronics Science and Engineering Center, Kyoto University, Kyoto 615-8510, Japan*

(Received 2 July 2008; revised manuscript received 25 September 2008; published 24 October 2008)

We report photoluminescence (PL) and Raman-scattering (RS) spectra in close-packed CdSe/Au mixed nanoparticle (NP) monolayers as a function of the ratio of CdSe to Au NPs in the film. The RS intensity showed slight enhancement with an increase in the Au NPs, while the PL intensity decreased dramatically. These results were explained by an energy-transfer (ET) model considering weak electromagnetic-enhancement factors estimated from the RS studies and ET rates from CdSe to Au NPs obtained from the time-resolved PL spectra.

DOI: [10.1103/PhysRevB.78.153308](https://doi.org/10.1103/PhysRevB.78.153308)

PACS number(s): 78.67.Bf, 73.21.La, 78.30.Fs

Remarkable progress in sample fabrication techniques has yielded well-controlled semiconductor and metal nanoparticles (NPs), which can be used as nanoscale building blocks, and unique optical properties of various nanostructured materials have been widely studied.^{1–6} Semiconductor NPs are one of the most promising materials because of their wavelength-tunable high-efficient photoluminescence (PL) owing to the quantum confinement effect. Great effort to develop various applications involving lasers, biolabeling, light-emitting diodes, and solar cells is currently under way.^{6–11} In the metal NPs a collective free-electron excited state, so-called localized surface plasmons, can be generated. The localized surface plasmons induce large localized electromagnetic fields, which enhance PL and Raman-scattering (RS) intensities of the materials in the vicinity of the metal nanostructures.^{12–17} However, it is also reported that the PL intensity is quenched because of the energy transfer (ET) from the luminescent materials to the metal nanostructures.^{15,18–20} Thus, the nature of the PL modification by plasmons is complex and is still an open question.

Recently, close-packed NP solids and macroscopically ordered NP solids have been successfully prepared and nanoscale ET processes have been actively studied.^{19–24} In particular, since the ratio of metal and semiconductor NPs in the films can be changed easily in close-packed metal-semiconductor mixed NP monolayers,²⁰ they make it possible to examine the influence of localized surface plasmons on the semiconductor NPs systematically. Thus, these closely packed metal-semiconductor mixed NP monolayers are expected to be one of the model samples that aid in understanding the electronic interaction between luminescent materials and localized surface plasmons. In the previous paper, we reported that the PL decay dynamics in the close-packed metal-semiconductor mixed NP monolayers are determined by the ET from the first- and second-neighbor CdSe (excitons) to Au NPs (plasmons).²⁰ However, the electromagnetic-field-enhancement or quenching effects on the PL intensity remain unclear in metal-semiconductor mixed NP monolayers. Since the RS studies give us information on enhanced localized electromagnetic fields induced by surface plasmons, one can discuss the electromagnetic-field-

enhancement effect on the PL properties.²⁵ Simultaneous measurements of the PL and RS spectra are expected to provide a further insight into ET processes behind the close-packed metal-semiconductor mixed NP monolayers.

In this Brief Report, we fabricated CdSe/Au mixed NP monolayers and measured their PL and RS spectra simultaneously in order to discuss the electromagnetic-field-enhancement effect on PL and ET processes. We found that the RS intensity showed slight enhancement with an increase in the Au NPs while the PL intensity decreased dramatically. The slight enhancement of the RS intensity and the dramatic decrease in the PL intensity were explained by considering the electromagnetic enhancement factors estimated from the RS studies and ET rates obtained from the time-resolved PL spectra.

The Au NPs were fabricated by a two-phase (toluene/water) reaction with a phase-transfer catalyst.²⁶ They were protected by 1-dodecanethiol and their diameter was about 5.8 nm. The CdSe/ZnS core/shell NPs (purchased from Evident Technologies) were used as CdSe NPs whose core diameter was about 5.2 nm. The CdSe/Au mixed NP monolayers were fabricated by a Langmuir-Blodgett (LB) method on a quartz substrate. Transmission electron microscope (TEM) images showed that the NPs in the LB films were almost close packed.²⁰ The number density of the CdSe NPs is defined as, $N = n_C / (n_C + n_A)$, where n_C and n_A are numbers of CdSe and Au NPs per unit area, respectively, obtained from the TEM images.

The absorption spectra of our sample were measured by using a monochromatic light of a tungsten lamp through a monochromator. The transmitted light from the sample was detected by a Si photodiode with a lock-in amplifier. For the simultaneous measurements of PL and RS spectra, a cw Ar-ion laser was used as the excitation light source. The excitation energy and the excitation power were 2.54 eV (488 nm) and 4.0 W/cm², respectively. The PL and RS spectra were measured in quasibackscattering geometry. A single monochromator with a liquid-nitrogen-cooled charge coupled device (CCD) camera was used for the PL measurements. The RS signal was dispersed by a triple monochromator (JOBIN YVON, SPEX1887) consisting of a filter and spectrograph

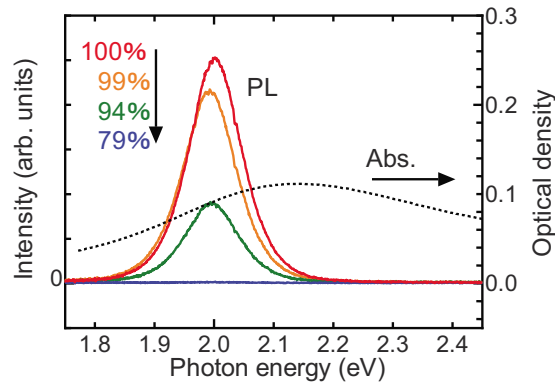


FIG. 1. (Color online) The PL spectra of various N (solid lines) and the absorption spectrum of $N=28\%$ (dotted line).

monochromators and detected by a liquid-nitrogen-cooled CCD camera. This experimental setup enables us to measure the PL and RS spectra simultaneously in the same sample spot with the same excitation laser. Thus, PL and RS signals can be compared directly. In addition, time-resolved PL was measured to study the PL dynamics of CdSe NPs. A second-harmonic wave (445–450 nm) of a cavity-dumped mode-lock Ti:sapphire laser was used as the excitation light source. The frequency and the pulse width were 544.77 kHz and about 150 fs, respectively. The excitation density was $0.26 \mu\text{J}/\text{cm}^2$. The time-resolved PL measurements were performed in quasibackscattering geometry with a single monochromator and a streak camera. The time resolution of this system was 180 ps. Since the excitation densities in both the PL and RS simultaneous measurements and time-resolved PL studies are sufficiently weak, it is not necessary to consider the exciton-exciton interaction between the photoexcited CdSe NPs. All the optical measurements mentioned above were performed at room temperature.

Figure 1 shows typical PL spectra of the samples of various N . In addition, the absorption spectrum of $N=28\%$ is shown by the dotted curve. The PL peak observed at ~ 2.0 eV is due to the excitons confined in the CdSe NPs. In the absorption spectrum, a broad absorption peak at ~ 2.1 eV is due to the surface plasmons of the Au NPs.²⁷ Since the absorption energy of the surface plasmons in the Au NPs and the exciton energy of the CdSe NPs are overlapped, it is expected that the Au and CdSe NPs interact with each other. It is noteworthy that the PL intensity decreases dramatically with an increase in the Au NP ratio. The significant decrease in PL intensity suggests that nonradiative decay processes due to the ET from CdSe to Au NPs are very efficient.²⁰

Figure 2(a) shows the PL decay curves of the $N=100\%$ and 91% samples. It is reported that the PL decay curves can be fitted by three exponential functions.²⁰ The PL decay curve of $N=100\%$ is approximately described by two exponential functions because it has the radiative recombination in CdSe NPs and ET between CdSe NPs. When N is large, the PL decay curves contain the same decay components of $N=100\%$ as well as the decay components of the ET from CdSe to Au NPs. In order to show the fast CdSe-Au and CdSe-CdSe-Au ET decay components in the measured decay

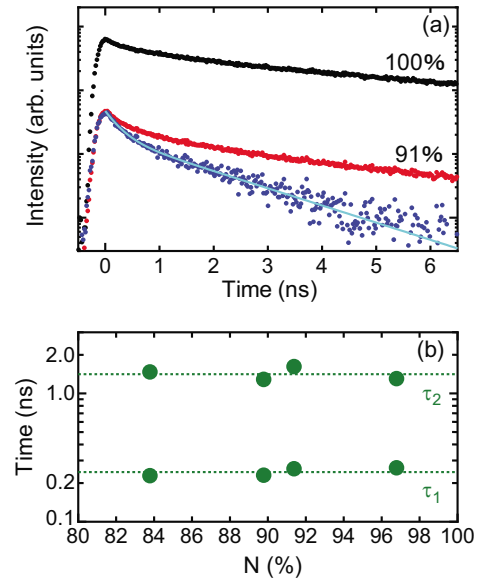


FIG. 2. (Color online) (a) The PL decay curves of $I(t, N=100\%)$ and $I'(t, N=91\%)$ with the fitted curve using two exponential functions. (b) The decay times obtained from $I'(t, N)$. The solid line indicates the fitted curve.

curves more clearly, we calculated $I'(t, N) = I(t, N) - kI(t, N=100\%)$, where $I(t, N)$ is the PL decay curve of N and k is a constant value so as to remove the longest decay component (the radiative recombination of excitons in CdSe NPs) from $I(t, N)$. Figure 2(a) also shows the calculated results of $I'(t, N=91\%)$, and the solid line indicates the fitted curve using two exponential functions. The two decay times, τ_1 and τ_2 ($\tau_1 < \tau_2$), were plotted in Fig. 2(b). Figure 2(b) shows that τ_1 and τ_2 are almost constant (0.24 and 1.4 ns, respectively) and do not depend on N .

Typical RS spectra of various N are shown in Fig. 3. The LO phonon peak of the CdSe NPs (Ref. 28) is observed at about 210 cm^{-1} [Fig. 3(a)]. In this figure, the background signals of the PL of the CdSe NPs and those of the RS of the quartz substrate were subtracted. Furthermore, to improve the signal-to-noise ratio, the RS spectra were measured three

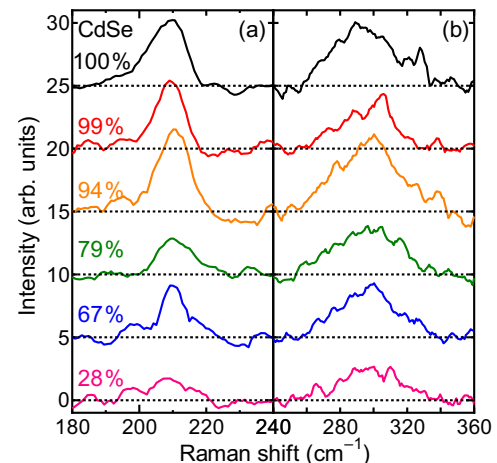


FIG. 3. (Color online) The RS spectra of (a) CdSe and (b) CdS-like LO phonons.

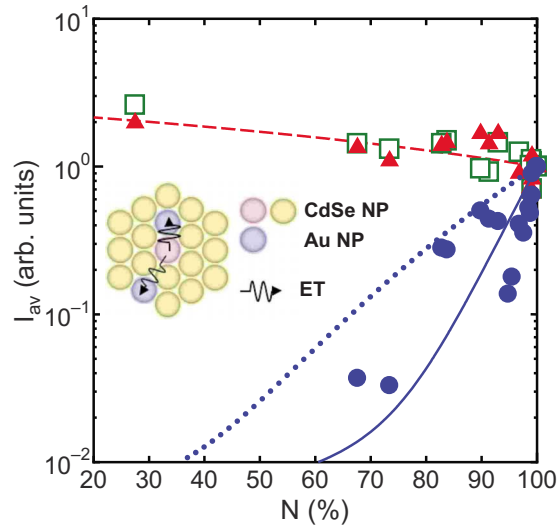


FIG. 4. (Color online) The spectrally integrated intensities per unit CdSe NP (I_{av}) of the PL and RS. The solid circles are PL intensities, and the solid triangles and open squares are CdSe and CdS-like RS intensities, respectively. The solid, broken, and dotted lines represent the calculated results (see text). The inset shows the close-packed NPs. The circle at the center is excited CdSe NP. The excited energy transfers to the first- or second-neighbor Au NPs as indicated by the arrows. All of the remaining circles are unexcited CdSe NPs.

times at the same position of the sample and they were averaged and smoothed numerically. In the RS spectra another peak was observed at about 300 cm^{-1} in all the films [Fig. 3(b)]. The LO phonon energy of the ZnS shell is 350 cm^{-1} (bulk),²⁹ which does not coincide with the observed peak energy. We found that the LO phonon energy of CdS is 305 cm^{-1} (bulk) (Ref. 30) and matches the observed peak energy. In the core/shell CdSe/ZnS NPs, there may be a Cd-S bonding at the interface between the CdSe core and the ZnS shell. The observed RS peak at 300 cm^{-1} may be due to this Cd-S bonding. Here, this signal is treated as CdS-like RS. Unlike the PL intensities, neither the CdSe nor the CdS-like RS intensity shows significant change.

Figure 4 shows the spectrally integrated PL and RS intensities per unit CdSe NP (I_{av}) as a function of N . Both integrated intensities are normalized at $N=100\%$. As shown in Fig. 4, the RS and the PL intensities have completely different behavior. The CdSe (solid triangles) and CdS-like RS intensities (open squares) increase slightly when Au NPs are increased. This result suggests that the local electromagnetic field is slightly enhanced. Even though the local electromagnetic field is enhanced, the PL intensity (solid circles) decreases dramatically. It is expected that the ET from the CdSe to Au NPs plays a dominant role in the change of PL intensity.

First, we will discuss the slight enhancement of RS intensity. Let us assume that the NPs are aligned to form a close-packed layer (inset of Fig. 4). Since the RS enhancement is weak, only the first-neighbor Au NPs are considered to enhance the CdSe RS intensity. There are six equivalent first-neighbor sites for each CdSe NP. When the number of the Au NPs located at the first-neighbor sites is l ($0 \leq l \leq 6$), the

enhanced RS factor is given by $\eta_{\text{Raman}}(l) = 1 + \alpha l$, where the enhancement factor for one pair of CdSe-Au NPs is defined as $1 + \alpha$ and each Au NP is assumed to enhance the RS intensity independently. The probability that the number of the Au NPs at the first-neighbor sites is l for given N can be written as ${}_6C_l(1-N)^l N^{6-l}$. Here, ${}_nC_l$ stands for combinations defined as ${}_nC_l = n! / \{l!(n-l)!\}$. Thus, the enhancement factor is derived as

$$S_{\text{Raman}}(N) = \sum_{l=0}^6 {}_6C_l(1-N)^l N^{6-l} \eta_{\text{Raman}}(l). \quad (1)$$

The enhancement factor $S_{\text{Raman}}(N)$ can be directly compared with I_{av} of the Raman intensity. The broken line in Fig. 4 shows the fitting result using Eq. (1). The fitting curve reproduces the experimental data well and α is estimated to be 0.24. For RS, the local electromagnetic enhancement affects the enhancement of both the incident and scattered fields. On the other hand, only the incident-field-enhancement affects the PL intensity. Thus, the electromagnetic enhancement factor for the PL intensity is $[\eta_{\text{Raman}}(l)]^{1/2}$ (Ref. 25) and the enhancement factor of one pair of CdSe-Au NPs $[\eta_{\text{Raman}}(1)]^{1/2} = 1.11$. This is consistent with the theoretically predicted value (~ 1.2), where the Au and CdSe NP radii are 6.5 and 3.75 nm, respectively, and the distance between their surfaces is 1 nm.³¹ Therefore, the estimated value of α is thought to be reasonable.

Next, we will discuss the significant decrease in PL intensity. The observed τ_1 and τ_2 correspond to ET of CdSe to first-neighbor Au NPs and to ET of CdSe to second-neighbor Au NPs through a stepwise process, respectively.²⁰ The ET rates can be obtained through the relation, $K_{\text{ET},i} = 1/\tau_i - 1/\tau_{\text{rad}}$ ($i=1, 2$), where τ_{rad} is the radiative lifetime, which is estimated to be 12.1 ns from the longest PL decay components in $N=100\%$. Since τ_1 and τ_2 are obtained in the high N region, $K_{\text{ET},1}$ and $K_{\text{ET},2}$ are regarded as CdSe-Au pair ET rates from a CdSe NP to first- and second-neighbor Au NPs, respectively. The numbers of equivalent sites for the first- and second-neighbor NPs are 6 and 12, respectively (inset of Fig. 4), similar to the discussion of RS enhancement. The probabilities that the numbers of the first- and second-neighbor Au NPs are l ($0 \leq l \leq 6$) and m ($0 \leq m \leq 12$) for given N are described as ${}_6C_l(1-N)^l N^{6-l}$ and ${}_{12}C_m(1-N)^m N^{12-m}$, respectively, and the PL efficiency is described as $\eta_{\text{PL}}(l, m) = K_{\text{rad}} / (K_{\text{rad}} + lK_{\text{ET},1} + mK_{\text{ET},2})$, where $K_{\text{rad}} = 1/\tau_{\text{rad}}$. Thus, the PL efficiency for the number density N is written as

$$S_{\text{PL}}(N) = \sum_{l=0}^6 \sum_{m=0}^{12} \sqrt{\eta_{\text{Raman}}(l)} {}_6C_l(1-N)^l N^{6-l} {}_{12}C_m(1-N)^m N^{12-m} \eta_{\text{PL}}(l, m). \quad (2)$$

In this equation, the electromagnetic-field-enhancement effect, $[\eta_{\text{Raman}}(l)]^{1/2}$, is taken into account. The PL efficiency $S_{\text{PL}}(N)$ can be directly compared with I_{av} of the PL intensity, and the solid line in Fig. 4 shows the calculated result of Eq. (2). The calculated and experimental results agree well without any fitting parameters. For comparison, the dotted line is

the calculated PL efficiency considering the direct ET of only the first-neighbor Au NPs, which does not agree with the experimental data. The CdSe NP number density dependence of the PL intensity also shows that PL properties in CdSe/Au mixed NP monolayers are determined by two ET processes: the direct ET from CdSe to the first-neighbor Au NPs and the stepwise ET from CdSe to second-neighbor Au NPs. In addition, we found that the PL intensity is increased only $\sim 1.5 \times 10^{-3}$ at $N=70\%$ due to the electromagnetic-field-enhancement effect and that the PL enhancement effect is very weak in our samples.

In summary, we fabricated CdSe/Au mixed NP monolayers and measured the PL and RS spectra simultaneously in order to investigate the influence of the PL and RS properties of semiconductor NPs on the surface plasmons of metal NPs. With an increase in the Au NP ratio, the PL intensity decreased dramatically while the RS intensity increased

slightly. The observed N dependences of the RS and PL intensities were explained by an ET model which considered the effects of electromagnetic enhancement and ET. It is clarified that the electromagnetic-field-enhancement effect is very weak and that the ET plays a dominant role in PL quenching. We have demonstrated that conducting simultaneous measurements of PL and RS is a useful technique to understand the interaction between metal and semiconductor nanostructures.

The authors would like to thank K. Hosoki of Kyoto University for the technical assistance with sample preparations, T. Teranishi for providing the Au NP samples, and H. Yanagi for helpful discussion. Part of this work was supported by JSPS KAKENHI (Contract No. 18540319), and Nippon Sheet Glass Foundation for Materials Science and Engineering.

*Corresponding author; aishi@ms.naist.jp

†Corresponding author; kanemitsu@scl.kyoto-u.ac.jp

¹L. Brus, J. Chem. Phys. **90**, 2555 (1986).

²C. B. Murray, D. J. Norris, and M. G. Bawendi, J. Am. Chem. Soc. **115**, 8706 (1993).

³Y. Kanemitsu, Phys. Rep. **263**, 1 (1995).

⁴C. B. Murray, C. R. Kagan, and M. G. Bawendi, Science **270**, 1335 (1995).

⁵A. P. Alivisatos, J. Phys. Chem. **100**, 13226 (1996).

⁶V. I. Klimov, J. Phys. Chem. B **110**, 16827 (2006).

⁷V. L. Colvin, M. C. Schlamp, and A. P. Alivisatos, Nature (London) **370**, 354 (1994).

⁸M. Bruchez, Jr., M. Moronne, P. Gin, S. Weiss, and A. P. Alivisatos, Science **281**, 2013 (1998).

⁹W. C. W. Chan and S. Nie, Science **281**, 2016 (1998).

¹⁰V. I. Klimov, A. A. Mikhailovsky, S. Xu, A. Malko, J. A. Hollingsworth, C. A. Leatherdale, H.-J. Eisler, and M. G. Bawendi, Science **290**, 314 (2000).

¹¹A. J. Nozik, Physica E (Amsterdam) **14**, 115 (2002).

¹²M. Moskovits, Rev. Mod. Phys. **57**, 783 (1985).

¹³S. Nie and S. R. Emory, Science **275**, 1102 (1997).

¹⁴K. Kneipp, Y. Wang, H. Kneipp, L. T. Perelman, I. Itzkan, R. R. Dasari, and M. S. Feld, Phys. Rev. Lett. **78**, 1667 (1997).

¹⁵K. T. Shimizu, W. K. Woo, B. R. Fisher, H. J. Eisler, and M. G. Bawendi, Phys. Rev. Lett. **89**, 117401 (2002).

¹⁶K. Okamoto, S. Vyawahare, and A. Scherer, J. Opt. Soc. Am. B **23**, 1674 (2006).

¹⁷Y. Ito, K. Matsuda, and Y. Kanemitsu, Phys. Rev. B **75**, 033309

(2007).

¹⁸E. Dulkeith, M. Ringler, T. A. Klar, J. Feldmann, A. M. Javier, and W. J. Parak, Nano Lett. **5**, 585 (2005).

¹⁹A. Ueda, T. Tayagaki, and Y. Kanemitsu, Appl. Phys. Lett. **92**, 133118 (2008).

²⁰K. Hosoki, T. Tayagaki, S. Yamamoto, K. Matsuda, and Y. Kanemitsu, Phys. Rev. Lett. **100**, 207404 (2008).

²¹C. R. Kagan, C. B. Murray, M. Nirmal, and M. G. Bawendi, Phys. Rev. Lett. **76**, 1517 (1996).

²²C. R. Kagan, C. B. Murray, and M. G. Bawendi, Phys. Rev. B **54**, 8633 (1996).

²³S. A. Crooker, J. A. Hollingsworth, S. Tretiak, and V. I. Klimov, Phys. Rev. Lett. **89**, 186802 (2002).

²⁴M. Achermann, M. A. Petruska, S. A. Crooker, and V. I. Klimov, J. Phys. Chem. B **107**, 13782 (2003).

²⁵A. Hartschuh, H. Qian, A. J. Meixner, N. Anderson, and L. Novotny, Nano Lett. **5**, 2310 (2005).

²⁶T. Shimizu, T. Teranishi, S. Hasegawa, and M. Miyake, J. Phys. Chem. **107**, 2719 (2003).

²⁷R. H. Doremus, J. Chem. Phys. **40**, 2389 (1964).

²⁸P. Y. Yu and J. E. Smith, Jr., Phys. Rev. Lett. **37**, 622 (1976).

²⁹R. E. Halsted, M. R. Lorenz, and B. Segall, J. Phys. Chem. Solids **22**, 109 (1961).

³⁰B. Tell, T. C. Damen, and S. P. S. Porto, Phys. Rev. **144**, 771 (1966).

³¹A. O. Govorov, G. W. Bryant, W. Zhang, T. Skeini, J. Lee, N. A. Kotov, J. M. Slocik, and R. R. Naik, Nano Lett. **6**, 984 (2006).